Hindawi
Advances in Materials Science and Engineering
Volume 2022, Article ID 2233443, 10 pages
https://doi.org/10.1155/2022/2233443

Research Article

Microstructural Features, Tensile Properties, and Impact Toughness of Linear Friction Welded High-Temperature Alloy Joints for Blisk Assembly Applications

C. Mukundhan,[1] **P. Sivaraj**,[1] **V. Balasubramanian**,[1] **Tushar Sonar**,[2] **Vijay Petley**,[3] **and Shweta Verma**[3]

[1]*Centre for Materials Joining and Research (CEMAJOR), Department of Manufacturing Engineering, Annamalai University, Annamalai Nagar, Chidambaram 608002, Tamil Nadu, India*
[2]*Department of Mechanical Engineering, G. S. Mandal's Maharashtra Institute of Technology, Aurangabad 431010, Maharashtra, India*
[3]*Materials Group (MTG), Gas Turbine Research Establishment (GTRE), Bengaluru 560093, Karnataka, India*

Correspondence should be addressed to Tushar Sonar; tushar.sonar77@gmail.com

Received 30 July 2022; Revised 11 August 2022; Accepted 22 August 2022; Published 24 September 2022

Academic Editor: Samson Jerold Samuel Chelladurai

The main objective of this investigation is to analyze the microstructure, tensile properties, and impact toughness of Ti6Al4V alloy joints developed using optimized parameters of linear friction welding (LFW) for gas turbine blisk assembly applications. The 6 mm thick plates of Ti6Al4V alloy were joined using a friction time of 40 sec, a friction pressure of 20 MPa, a forging pressure of 10 MPa, a forging time of 3 sec, and an oscillating frequency of 14 Hz. The different regions of joints were analyzed using a stereo zoom microscope. Optical and scanning electron microscope (SEM) was used for analysing the microstructural features of joints. The room temperature tensile properties, hardness, and impact toughness of LFW-Ti6Al4V alloy joints were evaluated and correlated to the microstructural features of weld region. The fractured sections of tensile and impact toughness specimens of joints were analyzed using SEM and the failure of joints was correlated with the hardness survey. Results showed that the LFW-Ti6Al4V alloy joints developed using the optimized parameters exhibited a tensile strength (TS) of 1015 MPa, a yield strength (YS) of 940 MPa, and an elongation (EL) of 8%. The joints revealed 98.54%, 95.91%, and 66.67% of tensile strength, yield strength, and ductility of the parent metal. The LFW joints disclosed impact toughness (IT) of 17.2 J which is 89.77% impact toughness of the parent metal. The superior tensile properties and impact toughness of LFW-Ti6Al4V alloy joints are mainly attributed to a greater degree of refinement of $\alpha + \beta$ grains in the weld interface, which offers greater resistance to tensile deformation and crack propagation.

1. Introduction

Ti6Al4V is an α+β titanium (Ti) alloy extensively used in automobile, aerospace, nuclear, and chemical industries [1]. It exhibits high corrosion resistance, high-temperature mechanical properties, and lower density [2]. It is principally used in the aero-engine blisk assembly [3]. Tungsten inert gas (TIG) welding is extensively used for joining titanium alloys [4, 5, 6]. The greater heat input of TIG welding causes coarsening of grain in the fusion zone microstructure, wider heat affected zone (HAZ), softening in HAZ, distortion, and weld metal contamination [7, 8, 9]. The greater energy density processes such as laser beam (LBW) [10, 11, 12] and electron beam (EB) welding [13, 14, 15] are also utilized to join Ti alloys. Nevertheless, a greater cooling rate in LBW and EBW causes problems such as cracking in weld metal and porosity defects [4, 16]. Solid-state welding (SSW) methods such as friction welding (FW) [17, 18, 19], friction stir welding (FSW) [20, 21, 22], and diffusion bonding (DB) [23, 24, 25] are extensively employed for developing similar and dissimilar joints of Ti alloys. Compared to different SSW processes, FW offers the benefits of enhanced joint

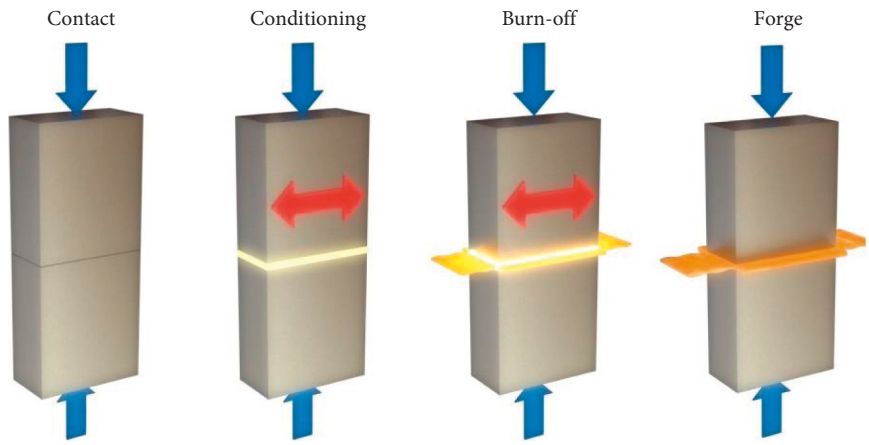

Figure 1: Four stages in linear friction welding [28].

efficiency, elimination of consumables, reduced processing time, and so on. Linear friction welding (LFW) is a type of FW process in which joints are developed by relative motion between joining surfaces and application of compressive forces [26]. In LFW, one joining surface will be kept stationary and the other joining surface is linearly oscillating. The heat is developed between joining surfaces due to friction and develops a plasticized zone at the joint interface during this process. After this, the final joint is produced by applying forging force with limited TMAZ (thermo-mechanically affected zone) [27]. The four stages in LFW process are shown schematically as shown in Figure 1.

Abbasi et al. [29] investigated the influence of filler metal on the microstructure and tensile performance of Ti6Al4V alloy joints. The joints produced with matching fillers exhibited higher tensile strength than others. Kishore Babu et al. [30] investigated the effects of current pulsing and PWHT (postweld heat treatment) on the microstructure and tensile properties of TIG weldments of Ti6Al4V alloy. The pulsing of current results in grain refinement of prior ß grains, which improves both ductility and strength of the weldments. Balasubramanian et al. [31] investigated the corrosion behaviour of pulsed gas tungsten arc welded joints and reported increases in corrosion resistance at increased levels of peak current and pulsing frequency up to a certain point. The greater refinement in the fusion zone (FZ) of joints was mainly responsible for the superior corrosion resistance of Ti alloy joints. Cao et al. [32] analyzed the influence of weld traverse speed on laser-welding of Ti6Al4V alloy joints. The existence of α' in FZ will increase hardness by 20% compared with a base metal. The microstructure is inhomogeneous in the weld joint, and the strength of the joint was found to be increased with a reduction in ductility. Romero et al. [33] analyze the influence of forging pressure on microstructure and the development of residual stress in LFW-Ti6Al4V joints and reported that forging pressure strongly influences weld width and TMAZ (thermo-mechanically affected zone). The weld interface (WI) and TMAZ experience temperatures exceeding the β transition temperature during LFW. Li et al. [34] studied the influence of friction time on the shape of flash and upset of LFW steel joints and stated that when upset length increases linearly, friction time also increases. The development of flash is in the friction direction with curved edges in the vertical direction. Effects of processing parameters were studied by Li et al. [35] through a numerical study. At higher oscillating frequencies, the temperature at the interface increases quickly, and shortening in the axial direction occurs faster. Similar behaviour is observed for friction pressure and amplitude. Mukundhan et al. [36] reported that tensile strength increases with an increase in forging pressure up to 10 MPa. Furthermore, an increase in forging pressure reduces the strength of joints. The strength of joints increases with an increase in friction time up to 40 s. Further increases in friction time reduce the strength of joints [19]. The tensile strength of joints is superior to an optimum level of oscillation frequency [37].

Table 1: Elemental composition of Ti6Al4V alloy (wt-%).

Al	V	Fe	O	C	N	H	Ti
6	4	0.19	0.15	0.06	0.04	0.01	Bal.

The reported literature shows that the research in LFW of Ti6Al4V alloy is mainly focused on studying the effects of amplitude, friction time, and forging pressure on microstructural features and the mechanical performance of joints. However, there is a lack of investigation on the analysis of the strength and impact toughness of LFW joints of Ti6Al4V alloy for the optimized condition of process parameters and its comparison to a base metal. Hence, the main objective of this investigation is to analyze the microstructure, tensile properties, and impact toughness of Ti6Al4V alloy joints developed using optimized parameters of LFW for blisk assembly applications.

2. Experimental Details

The rolled plates of Ti6Al4V alloy (6 mm thick) were used in this investigation for making the LFW joint. The elemental composition and mechanical properties of Ti alloy are reported in Tables 1 and 2. The plates were cut into the sizes of $40 \times 70 \times 6$ mm and $30 \times 60 \times 6$ mm using wire-cut EDM. A linear friction welding (LFW) machine (capacity: 20 kN) was employed for developing the joints. A photograph of the LFW machine is shown in Figure 2. The configuration and dimensions of the LFW-Ti6Al4V alloy joint are presented in

Table 2: Mechanical properties of Ti6Al4V alloy.

Tensile strength (MPa)	0.2% yield strength (MPa)	Elongation (%)	Microhardness (HV)	IT (J)>
1030	980	12	325	18

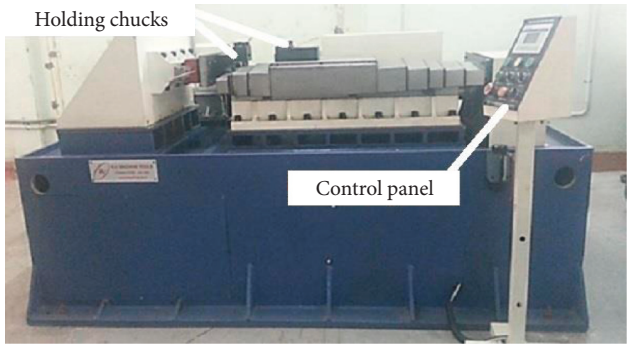

Figure 2: Photograph of the LFW machine used in this investigation.

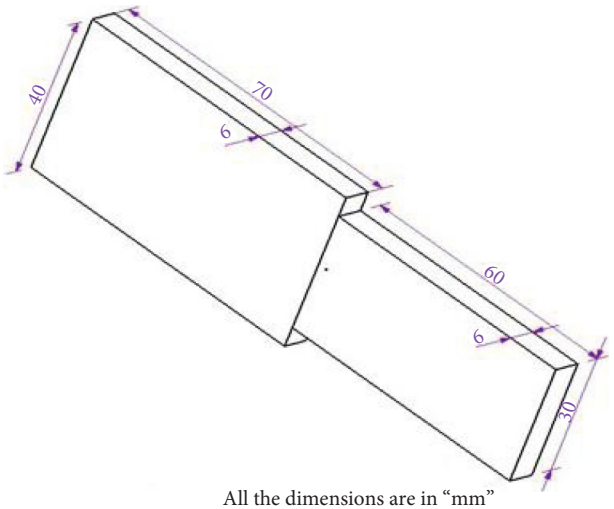

Figure 3: Dimensions of the LFW-Ti6Al4V alloy joint configuration.

Figure 3. The joints were developed using the optimized process parameters. The photograph of welded Ti6Al4V alloy joints is shown in Figure 4. Table 3 reports the optimized LFW parameters for joining 6 mm thick plates of Ti alloy. The tensile and impact toughness specimens were extracted from the joints as per the dimensions presented in Figures 5 and 6.

Tensile testing was done on LFW-Ti6Al4V joints utilizing a tensile testing machine as per the ASTM standard of E8/18. Tensile loading was applied at a strain rate of 2.4×10^{-3}/s. The microhardness survey was made across the joint cross-sectional area using Vicker's microhardness tester as per the ASTM standard of E384-17. Hardness was recorded at an interval of 0.2 mm along the weld interface (WI) and TMAZ (thermo-mechanically affected zone) region and at an interval of 0.5 mm in the HAZ (heat affected zone) and unaffected base metal (BM). The Charpy impact toughness was measured using the impact toughness machine as per the ASTM standard of E23. The testing was

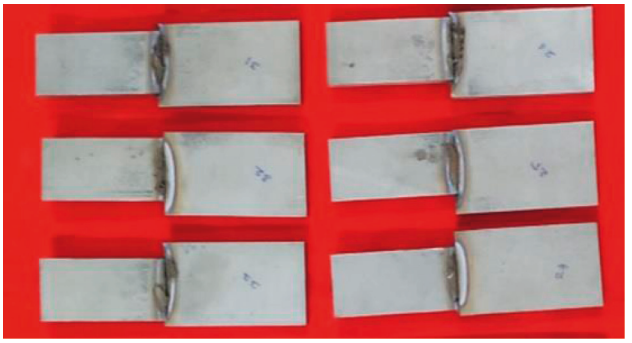

Figure 4: Photograph of fabricated LFW-Ti6Al4V joints.

Table 3: Optimized process parameters used to develop the joint.

Parameters	
Friction pressure (MPa)	20
Forging pressure (MPa)	10
Friction time (s)	40
Forging time (s)	3
Oscillating frequency (Hz)	14

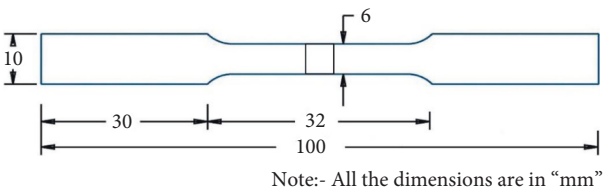

Figure 5: Dimensions of the tensile test specimen.

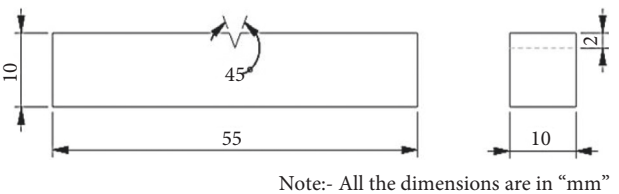

Figure 6: Dimensions of the impact toughness test specimen.

performed on 3 specimens, and the average was reported as the final value for tensile and impact toughness testing. The cross-section of the weld joint was polished and etched utilizing Kroll's reagent. The microstructural features of joints were analyzed using optical microscopy (OM) and scanning electron microscopy (SEM). The fractured test specimens were studied employing SEM.

3. Results and Discussion

3.1. Macrostructure and Microstructural Analysis. The optical and SEM micrograph of the Ti6Al4V alloy parent metal

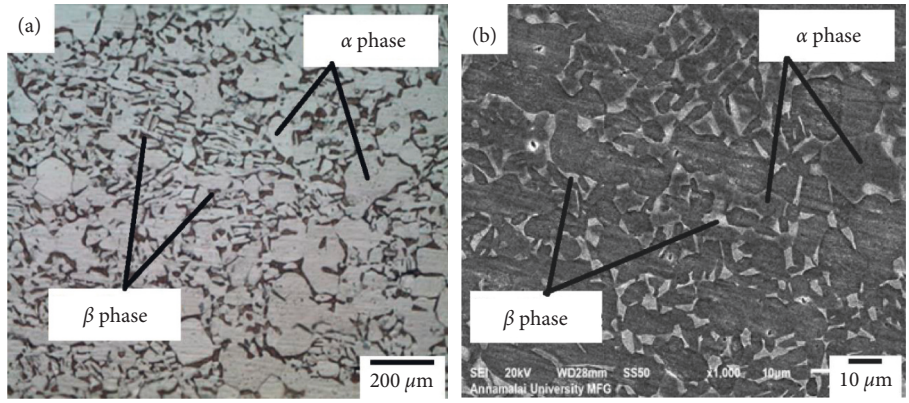

Figure 7: Micrograph of the unwelded Ti6Al4V alloy: (a) optical; (b) SEM.

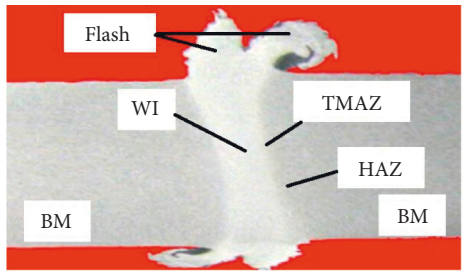

Figure 8: Macrograph of optimized LFW-Ti6Al4V alloy joints.

is shown in Figure 7. It consists of elongated α grains with an intergranular β phase. Figure 8 displays typical macrographs of LFW-Ti6Al4V joints. The joints were developed with any defects such as porosity, inclusions, blow holes, and cracks. The macrograph of the joint shows the distinct regions of the LF weld such as weld interface (WI), thermos-mechanically affected zone (TMAZ), heat affected zone (HAZ), and parent metal. These regions are characterized on the basis of grain size. The optical and SEM micrographs of the LFW-Ti6Al4V joint are shown in Figures 9 and 10. The WI region exhibited the evolution of finer $\alpha+\beta$ grains. The TMAZ region disclosed the evolution of coarser and highly deformed $\alpha+\beta$ grains that are oriented along the deformation direction. The HAZ was recorded to be much narrower in the LFW-Ti6Al4V joint. This makes it difficult to differentiate between the HAZ and the parent metal region. It is mainly due to the microstructural stability of the Ti6Al4V alloy below 600–800°C. The microstructural features can be much clearly seen in SEM micrographs. The WI zone is dynamically recrystalized. It exhibits microstructural deformation from the initial bimodal $\alpha+\beta$ microstructure to Widmanstätten morphologies along with the appearance of prior beta grains on the boundaries of Widmanstätten grains. The microstructural modification is correlated to the evolution of heat during LF welding at the joint interface. It causes the transformation of α phase into β phase. This microstructural modification in WI discloses that the temperature of frictional heat generated at the WI centre exceeds the β phase transformation temperature.

The microstructure of the weld interface is different compared to the parent metal. The prior bimodal α+β microstructure of the parent metal was evolved into a Widmanstätten microstructure outlined by prior β grain boundaries. The temperature generated due to frictional heating at the joint interface goes above the β -transus temperature of 995°C and results in the microstructural transformation into a single β phase. This causes progressive α to β phase transformation. The temperature at the weld centre is higher, and the evolution of prior β grains disclosed a complete α to β phase transformation. The temperature at the joint interface was reported up to 1100°C in the literature [38].

The important feature of the weld interface microstructure is the evolution of finer prior β grain microstructure. It is well reported in the literature that dynamic recovery and recrystallization occur by thermomechanical processing of the Ti6Al4V alloy above the β transus temperature. The microstructural evolution of the Widmanstätten structure is the result of cooling conditions after LFW. The transformed β grains from the single β phase region during rapid cooling (410°C/s) develop into a martensitic structure. It achieves the diffusionless transformation of β into α phase. Alternatively, during slower cooling, the transformed β grains from the single β phase region during rapid cooling (410°C/s) develop into α phase at β grain boundaries. The cooling rate influences the orientation and thickness of α plates. The rapid rate of cooling results in the evolution of multiorientated lamellae in the Widmanstätten microstructure. The slower rate of cooling results in the evolution of alpha lamellae arranged in packets or colonies. In this investigation, the evolution of Widmanstätten features of the transformed beta grains in the weld interface revealed a rapid cooling rate at the joint interface after LFW. The TMAZ consisted of a highly deformed $\alpha+\beta$ microstructure. It disclosed that the temperature in TMAZ did not cross the transformation temperature of β phase (995°C) [39].

3.2. Tensile Property of Welded Joints. The tensile properties of the LFW-Ti6Al4V joint are reported in Table 4, and it is compared with the parent metal. The tensile properties reported in this investigation were evaluated from the joints developed using the optimized LFW parameters. The tensile

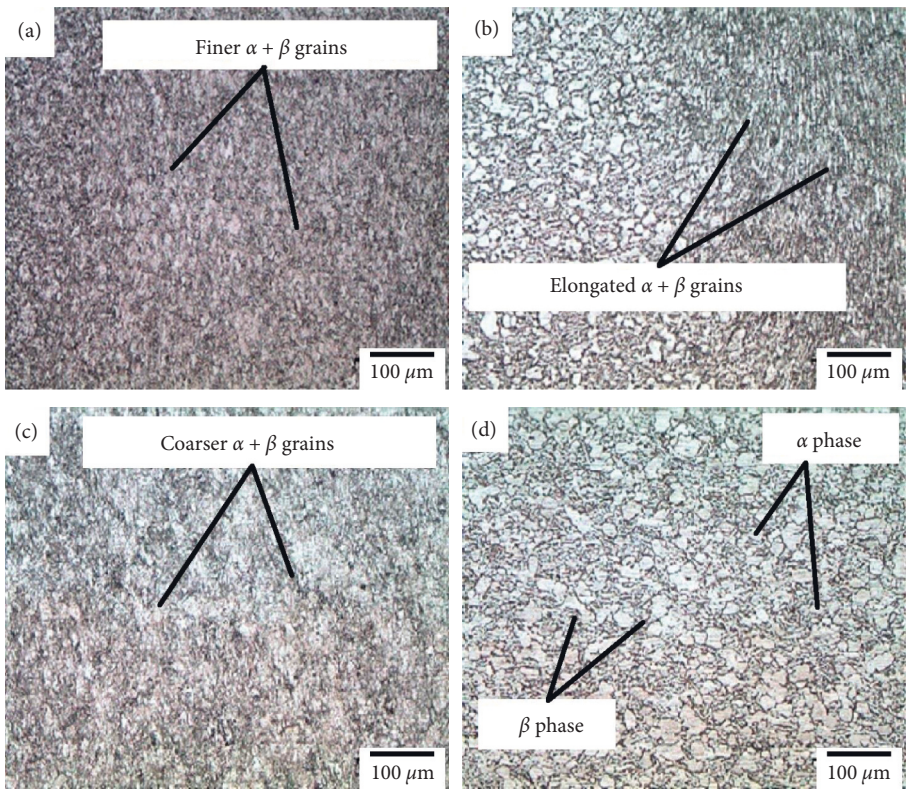

Figure 9: Optical micrograph of different regions of LFW-Ti6Al4V alloy joint: (a) weld interface; (b) TMAZ; (c) HAZ, and (d) unaffected parent metal.

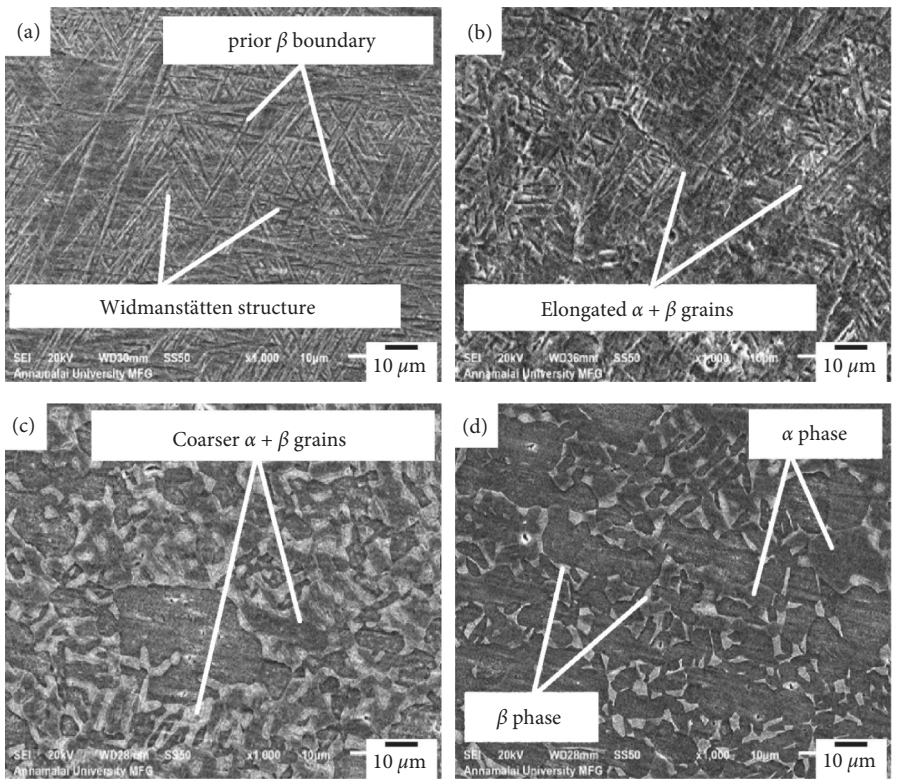

Figure 10: SEM micrograph of different regions of LFW-Ti6Al4V alloy joint: (a) weld interface; (b) TMAZ; (c) HAZ, and (d) unaffected parent metal.

Table 4: Tensile properties of LW-Ti6Al4V alloy joints.

Tensile strength (MPa)	0.2% yield strength (MPa)	Elongation (%)	Joint efficiency (%)	Fracture region
1015	926	8	98	TMAZ

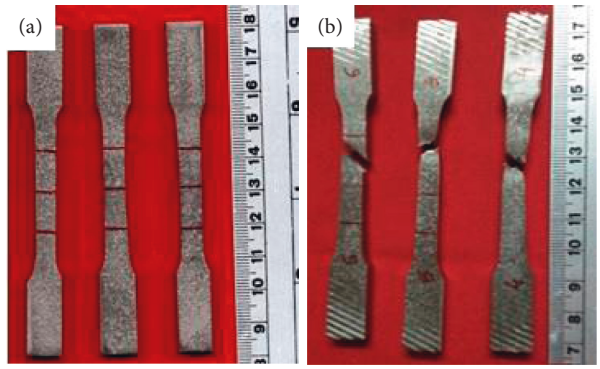

Figure 11: Photograph of tensile specimens: (a) before testing; (b) after testing.

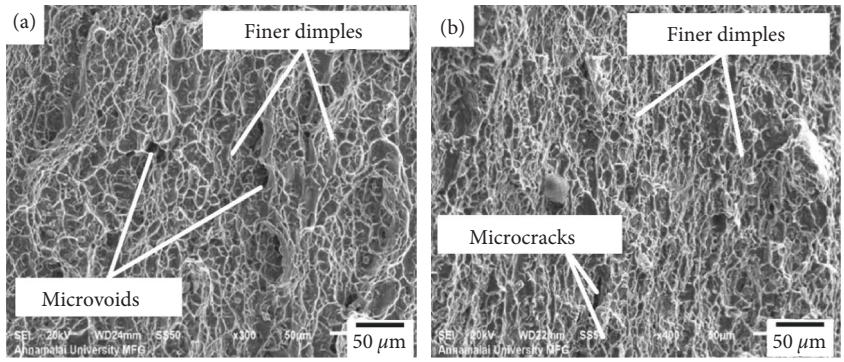

Figure 12: SEM fractographs of fractured tensile specimen.

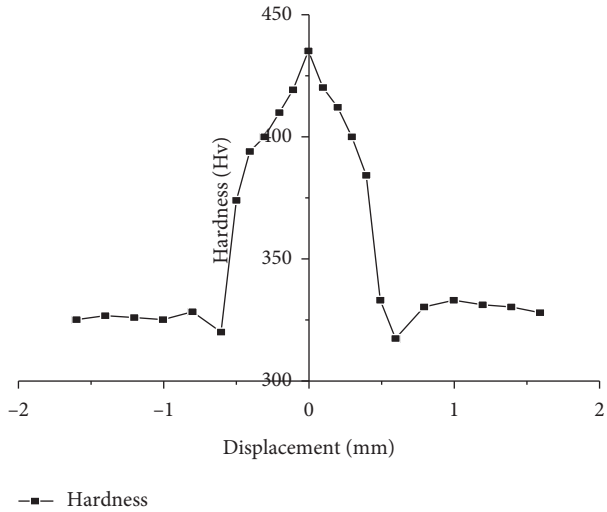

Figure 13: Microhardness distributions across the weld joint.

specimen photographs are displayed in Figure 11. The LFW-Ti6Al4V joints failed in the TMAZ region. The tensile failure of joints is correlated to the evolution of coarsened and plastically deformed oriented grains. This region provides less plastic deformation during tensile loading and offers easy crack initiation and propagation path. The tensile test results revealed that the LFW-Ti6Al4V joint exhibited a tensile strength of 1011 MPa, which is 98% of the parent metal strength. The yield strength of the joints was 926 MPa, which is 95.91% of the base metal yield strength. The tensile elongation of joints was 7.9% which is 66.67% of base metal ductility. The results reported in this investigation are superior to the results reported in the literature for fusion welding of Ti6Al4V alloy joints. It is mainly due to the reduced microstructural inhomogeneity across the different regions of the weld joint, the evolution of much finer grains in the WI region, and narrower HAZ. The SEM fractographs of tensile specimens are shown in Figure 12. The fractographs revealed finer dimples with an elongated morphology.

Table 5: Mean microhardness of different regions of joints.

Zones	Mean microhardness (HV)
WI	430
TMAZ	317
HAZ	325

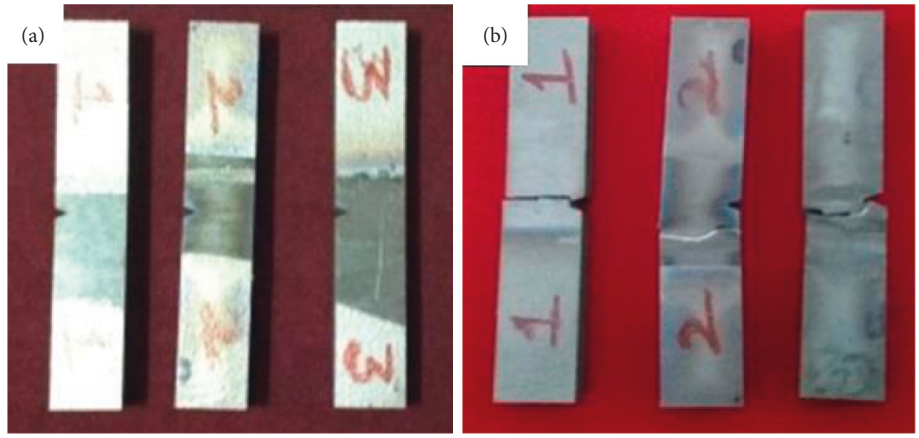

Figure 14: Photograph of impact toughness specimens.

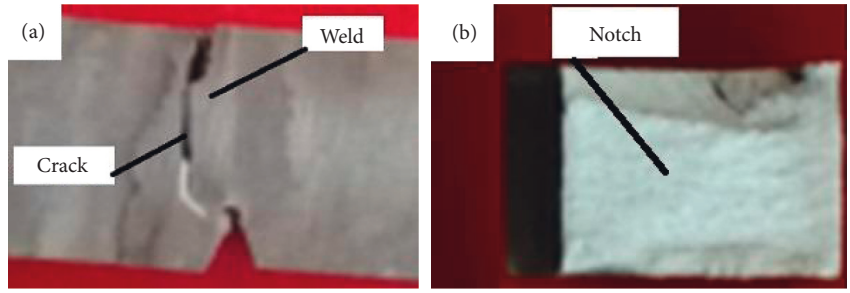

Figure 15: Macrograph of fractured sample after the impact toughness test: (a) front view; (b) cross-sectional view.

3.3. Microhardness. Figure 13 shows the microhardness distribution of LW-Ti6Al4V joints recorded from the centre of WI. The mean microhardness of different regions of joints is reported in Table 5. The WI disclosed the average hardness of 430 HV which is 32.30% greater than the parent metal. The microhardness was recorded to be much higher up to 450 HV at the WI centre. It is due to the evolution of much finer α+β grains. The lowest hardness of 315 HV was recorded in TMAZ due to grain coarsening which is mainly responsible for joint failure in this region. As the HAZ was much narrower, the hardness was varied in the HAZ, and the parent metal was not observed. The TMAZ showed a 4.61% lower hardness than the parent metal.

3.4. Impact Toughness. The photographs of the tested specimens are shown in Figure 14. The macrograph of the tested sample in closer view is shown in Figure 15. The impact toughness results of LFW-Ti6Al4V joints are reported in Table 6. It was reported as an average of three. The results showed that the LFW-Ti6Al4V joint exhibited an impact toughness of 16.2 J which is 60% of parent metal impact toughness. The SEM fractographs of fractured impact toughness test specimens are presented in Figure 16. The test specimens failed in the region of parent metal. This implies that WI regions exhibited superior toughness than parent metal owing to greater grain refinement in WI. The lowest value of impact toughness was recorded to be 15 J, and the highest value was 17.5 J. The fractographs showed that the crack was initiated in WI and rapidly passed through TMAZ towards the parent metal. The fractography of the sample revealed three different regions, i.e., a thinner fibrous zone close to the notch, a radiation zone along the middle, and a shear lip zone over the other three sides, respectively.

Table 6: Impact toughness test results of joints.

Joint no.	Impact toughness (J)	Average impact toughness (J)
1.	15	
2.	16	16.2
3.	17.5	

Apart from these zones, crack initiation zone (CIZ), crack propagation zone (CPZ), and shear failure were also located in these 3 zones. Also, some tearing ridges, planes of cleavage, and secondary cracks were observed at the CIZ. Near WI, finer dimples and tear ridges were evolved, which revealed a ductile fracture. In TMAZ, the quasicleavage fracture was observed. In addition to this, a cleavage mode of the fracture obtained in the weld interface crack initiation zone was due to the increased rate of loading during an impact test. Further analysis of fractography revealed plastic deformation and the formation of secondary cracks in the cleavage region due to the presence of superfine microstructure in WI, which yielded good elongation and better resistance to crack propagation. It drives the cracks to pass from WI into the parent metal. The analysis of CPZ revealed the quasicleavage mode of the fracture, showing both ductile and cleavage fractures. The brittle regions of the quasicleavage zone consisted of tearing ridges as well as deformed dimples. The shear-lip location exhibited a classical ductile

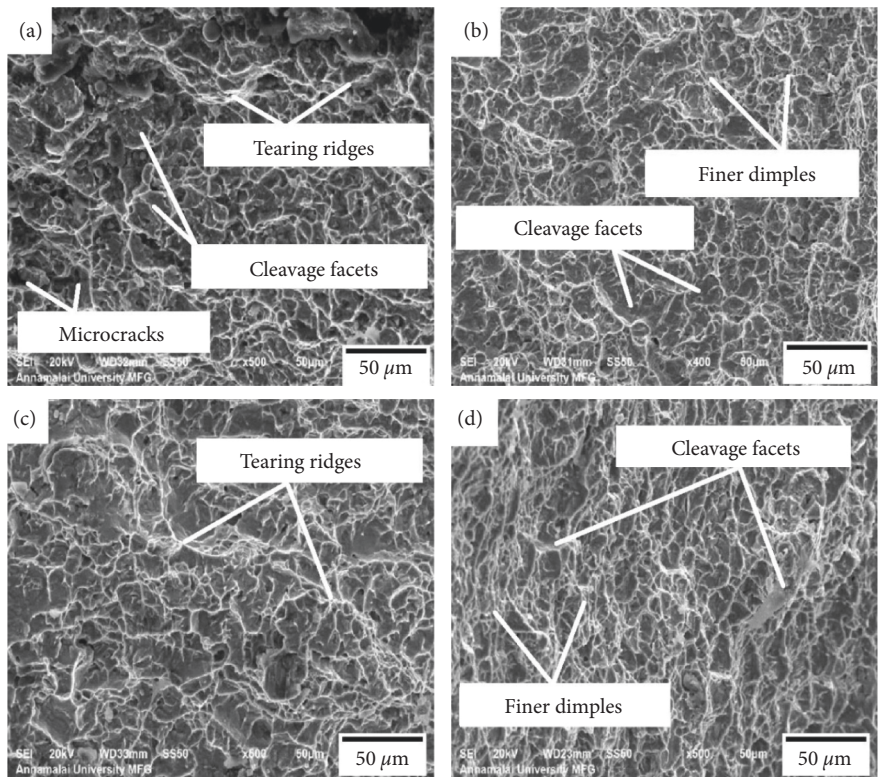

Figure 16: SEM fractographs of different regions of the impact toughness specimen of the LFW joint: (a) crack initiation zone; (b) crack propagation zone; (c) border of crack propagation and shear lip zone; (d) shear lip zone.

fracture mode with finer dimples dispersed in this zone. But at the near edges of the crack propagation area and shear-lip location, evidence of tear ridges and secondary cracks was seen, which exposed the composite mode of the cleavage fracture and the presence of dimples.

4. Conclusions

(1) The plates of Ti6Al4V alloy were joined successfully using linear friction welding without the defects of fusion welding in joining this alloy such as porosity, blow holes, solidification cracking, and contaminations.

(2) The LFW-Ti6Al4V alloy joints developed using the friction pressure of 20 MPa, frequency of 14 Hz, friction time of 40 s, and forging pressure of 10 MPa disclosed a greater tensile strength of 1015 MPa, yield strength of 940 MPa, and ductility of 8%.

(3) The LFW-Ti6Al4V alloy joints revealed 98.54%, 95.91%, and 66.67% of tensile strength, yield strength, and ductility of the parent metal.

(4) The LFW-Ti6Al4V alloy joints disclosed the impact toughness of 17.2 J which is 70% of base metal impact toughness.

(5) The superior tensile properties and impact toughness of LFW-Ti6Al4V alloy joints are mainly attributed to the greater degree of refinement of $\alpha + \beta$ grains in the weld zone which offers greater resistance to tensile deformation and crack propagation.

Data Availability

All data that support the findings of this study are included within the article.

Conflicts of Interest

The authors declare that they have no conflicts of interest.

Acknowledgments

The authors express gratitude to the Director of the Gas Turbine Research Establishment (GTRE), DRDO, Bangalore, for their support in carrying out this investigation.

References

[1] Y. Fan, W. Tian, Y. Guo, Z. Sun, and J. Xu, "Relationships among the microstructure, mechanical properties, and fatigue behavior in thin Ti6Al4V," *Advances in materials Science and Engineering*, vol. 2016, Article ID 7278267, 9 pages, 2016.

[2] X. Fang, L. Liu, J. Lu, and Y. Gao, "Optimization of forging process parameters and prediction model of residual stress of Ti-6Al-4V alloy," *Advances in Materials Science and Engineering*, vol. 2021, Article ID 3105470, 11 pages, 2021.

[3] A. Arun, .A Negemiya, N. Shankar et al., "Investigation on processing maps of diffusion bonding process parameters for Ti-6Al-4 V/AISI304 dissimilar joints," *Advances In Materials Science And Engineering*, vol. 2021, Article ID 5601970, 9 pages, 2021.

[4] X. L. Gao, L. J. Zhang, J. Liu, and J. X. Zhang, "A comparative study of pulsed Nd:YAG laser welding and TIG welding of thin Ti6Al4V titanium alloy plate," *Materials Science and Engineering A*, vol. 559, pp. 14–21, 2013.

[5] A. B. Short, "Gas tungsten arc welding ofα+βtitanium alloys: a review," *Materials Science and Technology*, vol. 25, pp. 309–324, 2009.

[6] T. S. Balasubramanian, M. Balakrishnan, V. Balasubramanian, and M. M. Manickam, "Influence of welding processes on microstructure, tensile and impact properties of Ti-6Al-4V alloy joints," *Transactions of Nonferrous Metals Society of China*, vol. 21, pp. 1253–1262, 2011.

[7] T. Sonar, V. Balasubramanian, S. Malarvizhi, T. Venkateswaran, and D. Sivakumar, "Effect of heat input on evolution of microstructure and tensile properties of gas tungsten constricted arc (GTCA) welded inconel 718 alloy sheets," *Metallography, Microstructure, and Analysis*, vol. 9, pp. 369–392, 2020.

[8] T. Sonar, V. Balasubramanian, S. Malarvizhi, A. Nagar, T. Venkateswaran, and D Sivakumar, "Microstructural characteristics and tensile properties of gas tungsten constricted arc (GTCA) welded Inconel 718 superalloy sheets for aeroengine components," *Materials Testing*, vol. 62, pp. 1099–1108, 2020.

[9] T. Sonar, S. Malarvizhi, and V. Balasubramanian, "Influence of arc constriction current frequency on tensile properties and microstructural evolution of tungsten inert gas welded thin sheets of aerospace alloy," *Transactions of Nonferrous Metals Society of China*, vol. 31, pp. 456–474, 2021.

[10] P. O. Omoniyi, R. M. Mahamood, N. Arthur et al., "Joint integrity evaluation of laser beam welded additive manufactured Ti6Al4V sheets," *Scientific reports*, vol. 12, no. 1, pp. 1–9, 2022.

[11] J. Chen, Z. Ouyang, X. Du, and Y. Wei, "Weld pool dynamics and joining mechanism in pulse wave laser beam welding of Ti-6Al-4V titanium alloy sheets assembled in butt joint with an air gap," *Optics & Laser Technology*, vol. 146, Article ID 107558, 2022.

[12] A. Squillace, U. Prisco, S. Ciliberto, and A. Astarita, "Effect of welding parameters on morphology and mechanical properties of Ti–6Al–4V laser beam welded butt joints," *Journal of Materials Processing Technology*, vol. 212, pp. 427–436, 2012.

[13] S. Wang and X. Wu, "Investigation on the microstructure and mechanical properties of Ti–6Al–4V alloy joints with electron beam welding," *Materials and Design*, vol. 36, pp. 663–670, 2012.

[14] J. Kar, S. K. Roy, and G. G. Roy, "Influence of beam oscillation in electron beam welding of Ti-6AL-4V," *International Journal of Advanced Manufacturing Technology*, vol. 94, no. 9-12, pp. 4531–4541, 2018.

[15] J. L. Barreda, F. Santamarıa, X. Azpiroz, A. M. Irisarri, and J. M. Varona, "Electron beam welded high thickness Ti6Al4V plates using filler metal of similar and different composition to the base plate," *Vacuum*, vol. 62, pp. 143–150, 2001.

[16] T. Sonar, V. Balasubramanian, S. Malarvizhi, T. Venkateswaran, and D. Sivakumar, "An overview on welding of Inconel 718 alloy - effect of welding processes on microstructural evolution and mechanical properties of joints," *Materials Characterization*, vol. 174, Article ID 110997, 2021.

[17] Y. Guo, M. M. Attallah, Y. Chiu, H. Li, S. Bray, and P. Bowen, "Spatial variation of microtexture in linear friction welded Ti-6Al-4V," *Materials Characterization*, vol. 127, pp. 342–347, 2017.

[18] J. W. Choi, Y. Aoki, K. Ushioda, and H. Fujii, "Linear friction welding of Ti-6Al-4V alloy fabricated below β-phase transformation temperature," *Scripta Materialia*, vol. 191, pp. 12–16, 2021.

[19] C. Mukundhan, P. Sivaraj, V. Petlay, S. Verma, and V. Balasubramanian, "Investigation on the effect of friction time on microstructural characteristics and mechanical properties of linear friction welded Ti-6Al-4V alloy joints," *journal of materials engineering and performance*, vol. 31, pp. 1–11, 2022.

[20] A. Fall, M. Jahazi, A. R. Khdabandeh, and M. H. Fesharaki, "Effect of process parameters on microstructure and mechanical properties of friction stir-welded Ti–6Al–4V joints," *International Journal of Advanced Manufacturing Technology*, vol. 91, pp. 2919–2931, 2017.

[21] S. Mironov, Y. Zhang, Y. S. Sato, and H. Kokawa, "Development of grain structure in β-phase field during friction stir welding of Ti–6Al–4V alloy," *Scripta Materialia*, vol. 59, pp. 27–30, 2008.

[22] J. Li, Y. Shen, W. Hou, and Y. Qi, "Friction stir welding of Ti-6Al-4V alloy: friction tool, microstructure, and mechanical properties," *Journal of Manufacturing Processes*, vol. 58, pp. 344–354, 2020.

[23] T. Li, L. Zhong, H. Wu, D. An, X. Li, and J. Chen, "Microstructure evolution and fatigue crack growth of diffusion bonded Ti-6Al-4V titanium alloy," *Journal of Alloys and Compounds*, vol. 918, Article ID 165816, 2022.

[24] Y. Chen, G. Wang, Y. Liu, L. Zhan, H. Diao, and Y. Wang, "Diffusion bonding of Ti6Al4V at low temperature via SMAT," *Metals*, vol. 12, p. 94, 2022.

[25] A. Arun Negemiya, S. Rajakumar, and V. Balasubramanian, "High-temperature diffusion bonding of austenitic stainless steel to titanium dissimilar joints," *Materials Research Express*, vol. 6, Article ID 066572, 2019.

[26] H. T. Nu, L. P. Minh, and N. H. Loc, "A study on rotary friction welding of titanium alloy (Ti6Al4V," *Advances in Materials Science and Engineering*, vol. 2019, Article ID 4728213, 9 pages, 2019.

[27] A. R. McAndrew, P. A. Colegrove, C. Bühr, B. C. Flipo, and A. Vairis, "A literature review of Ti-6Al-4V linear friction welding," *Progress in Materials Science*, vol. 92, pp. 225–257, 2018.

[28] An Aries Industries Company, "Linear-friction-welding," 2022, https://www.acb-ps.com/en/technologies/linear-friction-welding.

[29] K. Abbasi, B. Beidokhti, and S. A. Sajjadi, "Microstructure and mechanical properties of Ti-6Al-4V welds using α, near-α and α+β filler alloys," *Materials Science and Engineering A*, vol. 702, pp. 272–278, 2017.

[30] N. Kishore Babu, S. Ganesh Sundara Raman, R. Mythili, and S. Saroja, "Correlation of microstructure with mechanical properties of TIG weldments of Ti–6Al–4V made with and without current pulsing," *Materials Characterization*, vol. 58, pp. 581–587, 2007.

[31] M. Balasubramanian, V. Jayabalan, and V. Balasubramanian, "Effect of pulsed gas tungsten arc welding on corrosion behavior of Ti–6Al–4V titanium alloy," *Materials & Design*, vol. 29, pp. 1359–1363, 2008.

[32] X. Cao and M. Jahazi, "Effect of welding speed on butt joint quality of Ti–6Al–4V alloy welded using a high-power Nd: YAG laser," *Optics and Lasers in Engineering*, vol. 47, pp. 1231–1241, 2009.

[33] J. Romero, M. Attallah, M. Preuss, M. Karadge, and S. E. Bray, "Effect of the forging pressure on the microstructure and

residual stress development in Ti–6Al–4V linear friction welds," *Acta Materialia*, vol. 57, pp. 5582–5592, 2009.

[34] W. Y. Li, T. J. Ma, S. Q. Yang et al., "Effect of friction time on flash shape and axial shortening of linear friction welded 45 steel," *Materials Letters*, vol. 62, pp. 293–296, 2008.

[35] W. Y. Li, T. J. Ma, and J. Li, "Numerical simulation of linear friction welding of titanium alloy: effects of processing parameters," *Materials & Design*, vol. 31, pp. 1497–1507, 2010.

[36] C. Mukundhan, P. Sivaraj, V. Petley, S. Verma, and V. Balasubramanian, "Effect of forging pressure on microstructural characteristics and tensile properties of linear friction welded Ti-6Al-4V alloy joints," *Materials Today Proceedings*, vol. 45, pp. 1144–1150, 2021.

[37] C. Mukundhan, P. Sivaraj, V. Petley, S. Verma, and V. Balasubramanian, "Effect of Oscillation Frequency on Microstructure and Tensile Properties of Linear Friction Welded Ti-6Al-4V Alloy Joints," in *Green Materials and Advanced Manufacturing Technology*CRC Press, Boca Raton, Florida, 2020.

[38] A. Heidarzadeh, S. Mironov, R. Kaibyshev et al., "Friction stir welding/processing of metals and alloys: a comprehensive review on microstructural evolution," *Progress in Materials Science*, vol. 117, Article ID 100752, 2021.

[39] P. Wanjara and M. Jahazi, "Linear friction welding of Ti-6Al-4V: processing, microstructure, and mechanical-property inter-relationships," *Metallurgical and Materials Transactions A*, vol. 36, pp. 2149–2164, 2005.